Synthesis, structure, ionochromic and cytotoxic properties of new 2-(indolin-2-yl)-1,3-tropolones

Yurii A. Sayapin[*1], Eugeny A. Gusakov[2], Inna O. Tupaeva[2], Alexander D. Dubonosov[*1], Igor V. Dorogan[2], Valery V. Tkachev[3], Anna S. Goncharova[4], Gennady V. Shilov[3], Natalia S. Kuznetsova[4], Svetlana Y. Filippova[4], Tatyana A. Krasnikova[2], Yanis A. Boumber[5,6], Alexey Y. Maksimov[4], Sergey M. Aldoshin[3] and Vladimir I. Minkin[2]

Full Research Paper

Address:
[1]Federal Research Centre the Southern Scientific Centre of the Russian Academy of Sciences, Rostov-on-Don 344006, Russian Federation, [2]Institute of Physical and Organic Chemistry, Southern Federal University, Rostov-on-Don 344090, Russian Federation, [3]Federal Research Center of Problems of Chemical Physics and Medical Chemistry of the Russian Academy of Sciences, Chernogolovka 142432, Russian Federation, [4]National Medical Research Center of Oncology, Rostov-on-Don 344037, Russian Federation, [5]Institute of Fundamental Medicine and Biology, Kazan (Volga Region) Federal University, Kazan 420008, Russian Federation and [6]O'Neil Comprehensive Cancer Center at University of Alabama at Birmingham, Department of Medicine, Section of Hematology/Oncology, Heersink School of Medicine, Birmingham, AL 35233, USA

Email:
Yurii A. Sayapin[*] - sayapinscience@gmail.com;
Alexander D. Dubonosov[*] - aled@ipoc.sfedu.ru

* Corresponding author

Abstract

The acid-catalyzed reaction of benzo[$e(g)$] derivatives of 2,3,3-trimethylindolenines with o-chloranil leads to new 2-(benzo[$e(g)$]indolin-2-yl)-5,6,7-trichloro-1,3-tropolones and 2-(benzo[$e(g)$]indolin-2-yl)-4,5,6,7-tetrachloro-1,3-tropolones. Based on the results of PBE0/6-311+G(d,p) calculations, the structural and energetic characteristics of the tautomeric forms of the obtained 1,3-tropolones were determined. The structure of 2-(3,3-dimethyl-3H-benzo[g]indolin-2-yl)-5,6,7-trichloro-1,3-tropolone was determined by X-ray diffraction analysis. The compounds obtained are capable of switching emission at 420–440 nm and 476–530 nm upon successive exposure to CN^- and Hg^{2+} ions in an acetonitrile solution. 2-(1,1-Dimethyl-1H-benzo[e]indolin-2-yl)-5,6,7-trichloro-1,3-tropolone exhibited high in vitro cytotoxic activity against A431 skin cancer and H1299 lung cancer cell lines.

Introduction

1,2-Benzoquinones represent unique building blocks for various classes of heterocyclic systems. Their structure depends on the reactivity of the initial heterocycles and 1,2-benzo-quinones, as well as on the reaction conditions. In the series of 2-methylquinolines [1], 2-methylquinoxalines [2], 2-methylquinazolinones [3], 2-methylbenzoxazinones [4], and 2-methylbenzoxa(thia)zoles [5] the interaction with sterically hindered 1,2-benzoquinones and 3,4,5,6-tetrachloro-1,2-benzoquinone proceeds with the expansion of the *o*-quinone ring and results in 2-hetaryl-substituted 1,3-tropolones **1** (Scheme 1), which exhibit antibacterial [4] and cytotoxic activity [6,7].

Existing approaches to the synthesis of 1,3-tropolone deriva-tives have a number of drawbacks, namely, limited synthesis methodology and low yields of the target compounds [8-15]. Over the past decade, only a few reports have been published [16,17].

Indole derivatives, including those with conjugated aromatic and alicyclic rings, are of considerable interest because of their diverse biological activities (antibacterial, antimicrobial, anti-cancer, antidiabetic, etc.) [18-22]. For this reason, the synthetic goal of this work is to obtain heterocyclic indole compounds conjugated with a 1,3-tropolone moiety.

The variability of the products of acid-catalyzed reactions in the series of 2,3,3-trimethylindolenine with 1,2-benzoquinone de-rivatives depends on the nature of the substituents in the 1,2-benzoquinone. Thus, the interaction of 2,3,3-trimethylindole-nine with 3,5-di(*tert*-butyl)-1,2-benzoquinone leads to the for-mation of indolo[1,2-*a*]indoline derivatives [23], while the pres-ence of a nitro group in 4,6-di(*tert*-butyl)-3-nitro-1,2-benzo-quinone the reaction with 2,3,3-trimethylindolenine leads to an

o-quinone ring contraction and the formation of 2-azabicyclic products and pyridino[1,2-*a*]benzo[*e*]indol-10,11-diones [24]. *o*-Chloranil was found to be the most efficient 1,2-benzo-quinone, which engages in *o*-quinone ring-expansion reactions with 2,3,3-trimethylindolenines to form hard-to-reach polychlo-rinated derivatives of 2-(indolin-2-yl)-1,3-tropolones [5]. Unlike the cross-aldol reaction of *o*-chloranil with methyl ke-tones [13-15], which is always accompanied by the removal of one of the chlorine atoms from the seven-membered ring, the acid-catalyzed reaction between methylene-active heterocyclic compounds and *o*-chloranil depends on the reaction conditions and can proceed with or without the inclusion of a dehydrochlo-rination stage and leads to 5,6,7-trichloro- or 4,5,6,7-tetra-chlorotropones, respectively [5,25].

The present work reports the synthesis of new 2-(indolin-2-yl)-1,3-tropolones by the reaction of *o*-chloranil with benzoan-nelated derivatives of 2,3,3-trimethylindolenine, a comprehen-sive evaluation of the structure of the compounds obtained using quantum chemical methods, X-ray diffraction analysis, two-dimensional correlation NMR spectroscopy, as well as in-vestigation of their ionochromic properties towards CN⁻ and Hg²⁺ ions and evaluation of in vitro cytotoxic activity against A431 skin cancer and H1299 lung cancer cell lines.

Results and Discussion

We found that boiling of equimolar amounts of benzannelated 2,3,3-trimethylindolenines **2a,b** and *o*-chloranil (**3**) (method A) in dioxane leads to the formation of trichlorosubstituted 1,3-tropolones **7a,b** as the main reaction products (Scheme 2). Heating **2a,b** in acetic acid with a two-fold excess of *o*-chlo-ranil (**3**) (method B) is accompanied by the formation of tetra-chlorosubstituted 1,3-tropolones **8a,b** (Scheme 2 and Support-ing Information File 1).
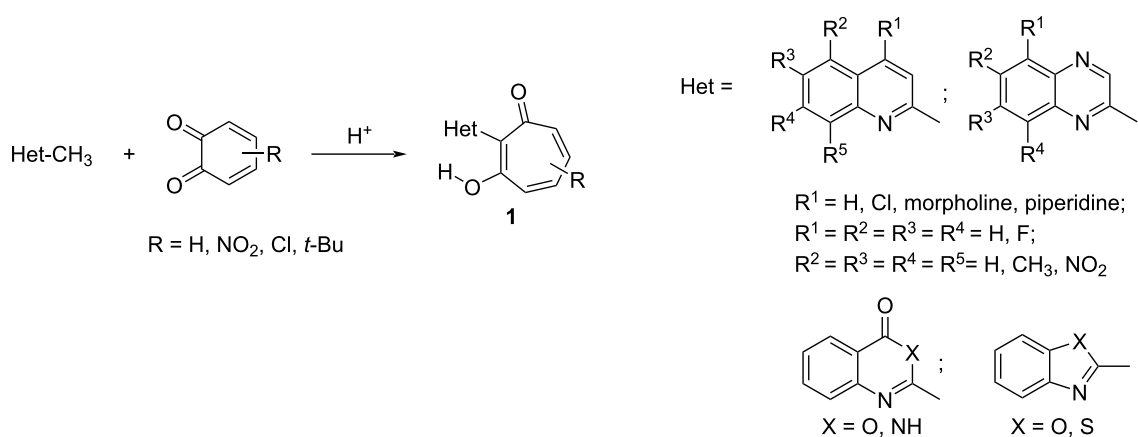
Scheme 1: Synthesis of 2-hetaryl-substituted 1,3-tropolones **1**.
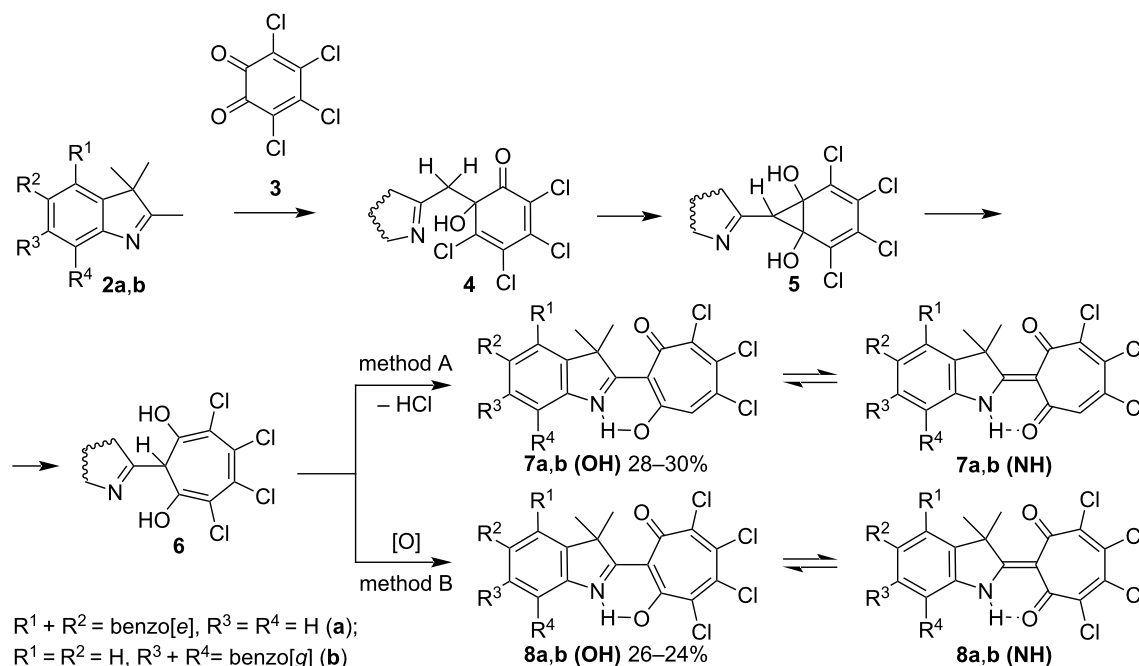
Scheme 2: Synthesis of 1,3-tropolones **7a,b** and **8a,b**. Reagents and conditions: method A: dioxane, reflux; method B: AcOH, 40–50 °C.

As shown in Scheme 2, in the initial step, the aldol condensation of 2,3,3-trimethylindolenine **2** with *o*-chloranil (**3**) leads to the intermediate compounds, 6-(2-hetarylmethylene)-6-hydroxy-2,4-cyclohexadien-1-ones **4**. Such intermediates were isolated preparatively and structurally characterized in the reactions of 2-methylquinolines with 3,5-di-(*tert*-butyl)-1,2-benzoquinone [1] and benzophenones with *o*-chloranil [15]. The norcaradiene derivatives **5**, formed in the next step by the intramolecular cyclization reaction of **4**, undergo thermal isomerization into 2,3-dihydrotropolones **6**. The formation of 2-(indolin-2-yl)-5,6,7-trichloro-1,3-tropolones **7a,b** is accompanied by dehydrochlorination of **6** upon boiling in dioxane according to method A. One of the conditions for carrying out the reaction according to method B is the use of a two-fold excess of quinone **3**. Oxidation of dihydrotropolones **6** with an excess of quinone **3** leads to the formation of 2-(indolin-2-yl)-4,5,6,7-tetrachloro-1,3-tropolones **8a,b** as final products. The detailed reaction mechanism in acetic acid solution was studied by the PBE0/6-311+G(d,p) method on the example of the interaction of 2-methylquinolines and 2-methylbenzazoles with 1,2-benzoquinone and *o*-chloroanil, respectively [1,25].

The structures of compounds **7** and **8** obtained by methods A and B were confirmed by ^{1}H NMR, IR spectroscopy and mass spectrometry (Supporting Information File 2). A distinctive feature of the ^{1}H NMR spectra of **7** in CDCl$_3$ is the signal of the tropolone ring proton, which appears at 6.9 ppm. A character-

istic specificity of the ^{1}H NMR spectra of compounds **7** and **8** is the presence of signals of hydroxy group protons forming a strong hydrogen bond with the indoline nitrogen atom, which closes the six-membered chelate cycle. These signals are observed in the weak field at 15.2–15.8 ppm for **7a,b** and 14.3–14.8 ppm for **8a,b**, respectively, as a broadened singlet peak.

A dynamic equilibrium of tautomeric forms **7, 8 (OH)–7, 8 (NH)** exists in solution, which can be detected by the broadening of the hydroxy group proton signal in the ^{1}H NMR spectrum (Scheme 2). The structures of tautomeric forms of **7a, 7b, 8a, 8b** and their energy characteristics were calculated by PBE0/6-311+G(d,p) method in the gas phase and polar solvent (DMSO) (Table 1, Figure 1 and Supporting Information File 3). According to the obtained data, the (**NH**) isomers of **7** and **8** are thermodynamically more stable than the corresponding (**OH**) forms. Increasing the polarity of the medium additionally enhances their stabilization. The introduction of an additional acceptor substituent to the tropolone moiety has a similar effect. In addition, compared to compounds **7a,b**, compounds **8a,b** show a marked increase in the intramolecular hydrogen bond length NH⋯O of the (**NH**) isomers and a decrease in the magnitude of hydrogen bond N⋯HO of the (**OH**) forms (Figure 1). On the other hand, the position of the benzoannelated fragment does not significantly affect the structural and energetic parameters of the studied compounds.

Table 1: Total energies with zero-point energy correction (E_{tot} + ZPE, a.u.) and relative energies (ΔE, kcal/mol) of (**NH**) and (**OH**) isomers of compounds **7** and **8** calculated by the PBE0/6-311+G(d,p) method in the gas phase (gas) and DMSO solution (sol).

compound	E_{tot} + ZPE(gas)	ΔE_{gas}	E_{tot} + ZPE(sol)	ΔE_{sol}
7a (**NH**)	–2392.806710	0	–2392.818223	0
7a (**OH**)	–2392.803386	2.1	–2392.812918	3.3
7b (**NH**)	–2392.809986	0	–2392.821048	0
7b (**OH**)	–2392.806819	2.0	–2392.816317	3.0
8a (**NH**)	–2852.269500	0	–2852.281433	0
8a (**OH**)	–2852.263504	3.8	–	–
8b (**NH**)	–2852.272654	0	–2852.284199	0
8b (**OH**)	–2852.266797	3.7	–	–
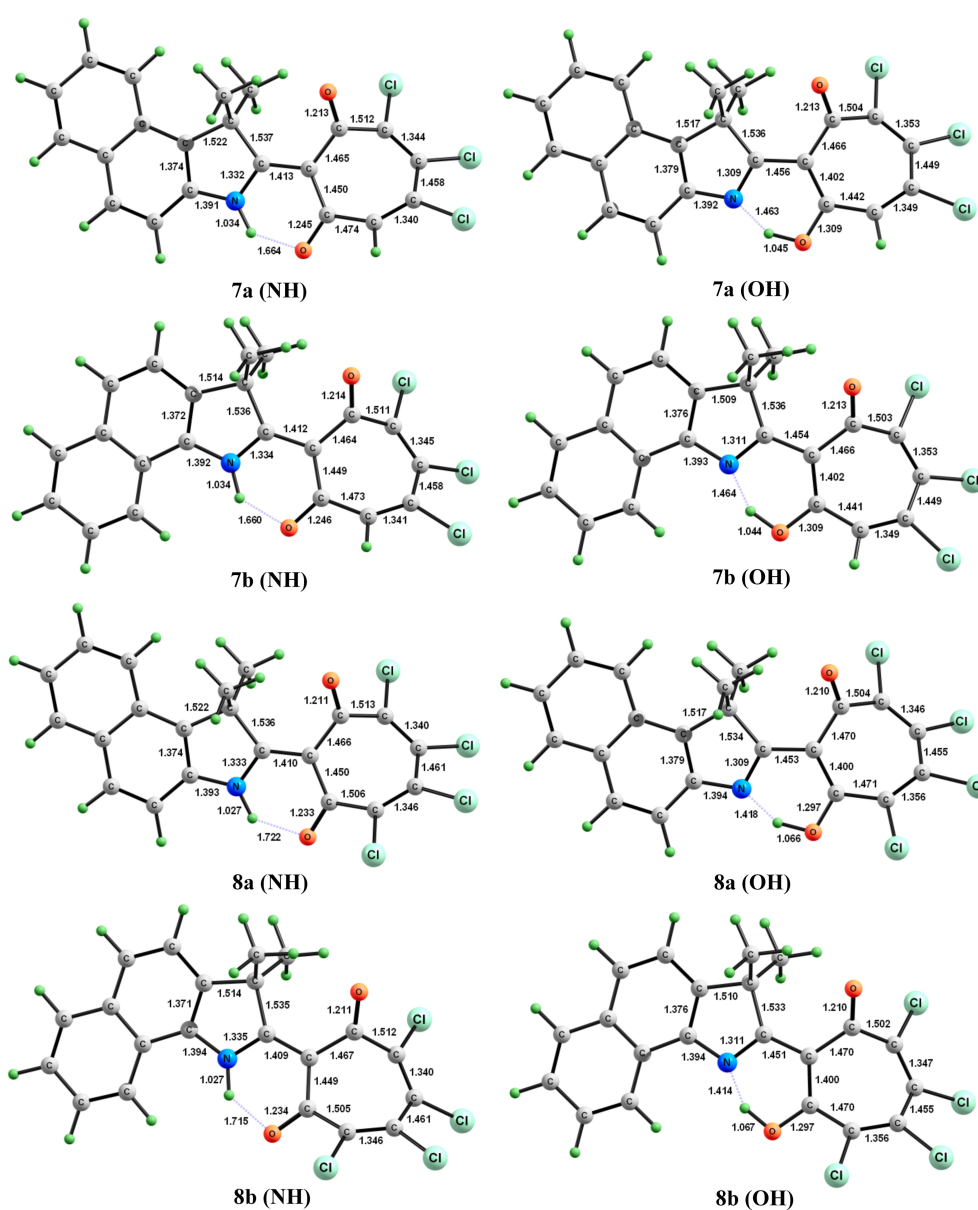
Figure 1: Structural characteristics of (**NH**) and (**OH**) tautomeric forms of compounds **7** and **8** in the gas phase according to PBE0/6-311+G(d,p) calculations. Bond lengths are given in Ångstrom.

The difference in the energy characteristics of the (**NH**) and (**OH**) tautomeric forms of compounds **7a**, **7b**, **8a**, and **8b** in the polar solvent and the gas phase is small (2.0–3.8 kcal/mol), and probably the nature of the solvent can influence the shift of the equilibrium towards one of the tautomeric forms.

To reveal the predominance of either the (**NH**) or (**OH**) tautomeric form of compounds **7a**, **7b**, **8a**, and **8b** in solution depending on the nature of the solvent, we carried out a detailed study using compound **7a**. A complete signal assignment of ^{1}H and ^{13}C NMR spectra was carried out, based on characteristic values of chemical shifts and cross-peak analysis in two-dimensional spectra of ^{1}H,^{1}H COSY correlations, as well as ^{1}H,^{13}C correlations HSQC, HMBC, and ^{1}H,^{15}N HMBC spectra in DMSO-d_6 and CDCl$_3$ (Supporting Information File 2).

In the ^{1}H NMR spectrum of **7a** in DMSO-d_6, the signal of the weak field proton is shifted to a stronger field of 14.23 ppm and appears as a narrow singlet (Supporting Information File 2, Figure S17). Analysis of two-dimensional correlation spectra of heteronuclear NMR spectroscopy shows that compound **7a** in DMSO-d_6 solution exists in the (**NH**) tautomeric form. Thus, in the ^{1}H,^{15}N HMBC spectrum of **7a** there are cross peaks of the indolenine nitrogen atom at 162.2 ppm with a weak field proton at δ_H 14.23 ppm, as well as aromatic protons H(4') and H(5') with δ_H 7.94 ppm and 7.97 ppm, respectively (Supporting Information File 2, Figure S19). In the two-dimensional ^{1}H,^{13}C HMBC spectrum of **7a**, a correlation of the NH proton with the bridging carbon atoms C(3a'), C(9b'), and the quaternary carbon atom C(1') of the indolenine fragment is observed with δ_H 136.6 ppm, 134.0 ppm, and 53.6 ppm, respectively (Supporting Information File 2, Figure S20). The most important HMBC correlations for the analysis of structure **7a** are schematically depicted in Figure 2.


Figure 2: Scheme of HMBC correlations of compound **7a** in DMSO-d_6.
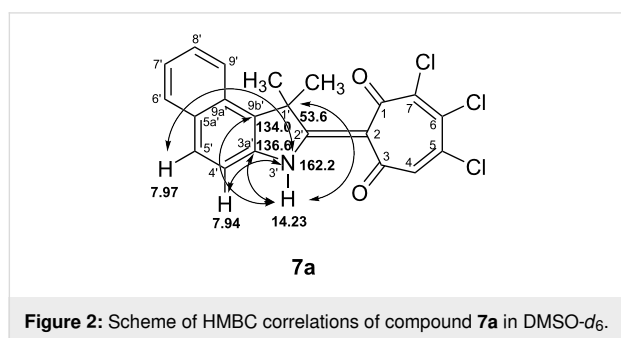
At the same time, in the ^{1}H,^{15}N HMBC spectra of **7a** in CDCl$_3$, there are no cross-peaks of the proton in the region of δ_H 15.15 ppm with the nitrogen atom of the indolenine fragment at 162.7 ppm, and in the ^{1}H,^{13}C HMBC spectrum, no correlations of the down-field proton with the carbon atoms of

the indolenine fragment are observed (Supporting Information File 2, Figures S21 and S22). Thus, in CDCl$_3$, compound **7a** is predominantly in the (**OH**) tautomeric form.

The structure of 2-(3,3-dimethyl-3*H*-benzo[*g*]indolin-2-yl)-5,6,7-trichloro-1,3-tropolone (**7b**) was established by X-ray diffraction analysis (Figure 3). The main distances and angles are summarized in Supporting Information File 3.

Figure 3: Molecular structure of 2-(3,3-dimethyl-3*H*-benzo[*g*]indolin-2-yl)-5,6,7-trichloro-1,3-tropolone (**7b**).
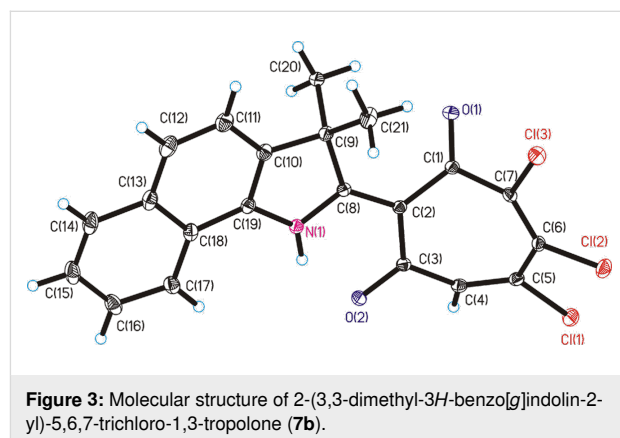
To compare the structural characteristics, we combined the molecule **7b** (solid lines) and the previously obtained 2-(3,3-dimethylindolin-2-yl)-5,6,7-trichloro-1,3-tropolone [5] (dashed lines) at the positions of N(1), C(2) and C(9) atoms (hydrogen atoms removed) (Figure 4).

Figure 4: Result of matching structures of **7b** (solid lines) and 2-(3,3-dimethylindolin-2-yl)-5,6,7-trichloro-1,3-tropolone (dashed lines) at the positions of N(1), C(2), and C(9) atoms.
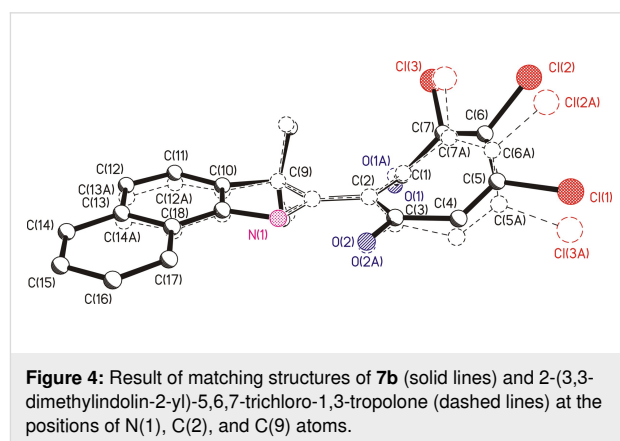
While maintaining the general configuration of the molecular framework, there are minor differences in the details of their structures, manifested in the observed distances between the atoms C12)···C(13A) = 0.31 Å, Cl(2)···Cl(2A) = 0.76 Å and in the geometric parameters of the tropolone rings. The angle between the planes C(2)C(3)C(6)C(7) and C(1)C(2)C(7) is equal to 42.9° (42.1°) (here and below, when comparing geometric values, similar values are given in parentheses for the previ-

ously obtained 2-(indolin-2-yl)-1,3-tropolone)). The angle between the planes C(2)C(3)C(6)C(7) and (3)C(4)C(5)C(6) is equal to 27.6° (34°). In compound **7b**, as in 2-(indolin-2-yl)-1,3-tropolone, an intramolecular hydrogen bond N(1)–H(1)···O(2) was realized with parameters: distances N–H = 0.86 (0.84) Å, H···O = 1.79 (1.83) Å, and N···O = 2.513 (2.518) Å, angle N–H–O 140.4° (138.0°).

The electronic absorption spectra of compounds **7a,b** and **8a,b** in acetonitrile have long wavelength bands in the region of 425–432 nm (Table 2). They exhibit dual-maxima fluorescence at 476–530 nm with normal and large Stokes shift values (Table 2, Figure 5).

This is consistent with the above conclusion about the existence of tautomeric equilibrium **7,8 (OH)–7,8 (NH)** in solutions based on NMR data and DFT quantum chemical calculations (Scheme 2). The emission with a larger Stokes shift

appears to correspond to the **7,8 (OH)** form and is caused by the excited-state intramolecular proton transfer (ESIPT) process due to intramolecular O→N proton migration in the singlet excited state [26,27].

The ionochromic sensitivity of compounds **7a,b** and **8a,b** to anions was investigated in acetonitrile upon addition of tetra-*n*-butylammonium salts (TBAX: F, Cl, Br, I, CN). Exclusively cyanide and fluoride anions lead to a naked-eye effect due to a change of the solution's colour from yellow-orange to pale yellow (Figure 5). At the same time, a new fluorescence band appears at 420–440 nm. The Stokes shifts of fluorescence decrease to normal values of 1800–2000 cm^{-1}, indicating a complete inhibition of the ESIPT process. These spectral transformations are usually caused by the formation of a strong N–H(O–H)···CN$^-$ (F$^-$) hydrogen bond up to deprotonation [28]. Using the principle of "relay recognition" [29], we investigated the sensitivity of in situ obtained complexes **9** and **10** with CN$^-$

Table 2: Absorption and fluorescence spectral data of compounds **7a,b** and **8a,b** in CH$_3$CN.[a]

compound	absorption, λ$_{max}$, nm (ε, L mol^{-1} cm^{-1})	fluorescence, λ$_{max}$, nm (*I*$_{fl}$, rel. units)	Stokes shift, (Δν$_{fl}$, cm^{-1})
7a	276 (17200), 300 (18400), 427 (20400)	485 (260), 520 (180)	2800, 4200
7b	292 (14000), 432 (19100)	495 (220), 523 (190)	2950, 4050
8a	300 (14800), 310 (15200), 418 (20000)	476 (420), 520 (190)	2900, 4700
8b	300 (14400), 425 (21900)	491(480), 530 (250)	3150, 4650

[a]*I*$_{fl}$ – the relative fluorescence intensity; *c* 2.5 × 10^{-5} mol L^{-1}, λ$_{ex}$ 417 nm, PMT voltage 940 V.
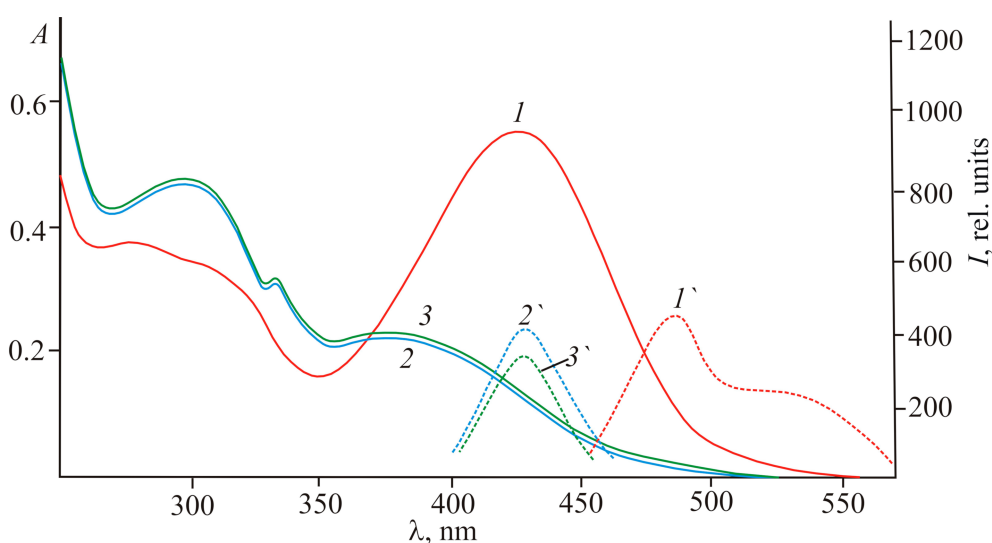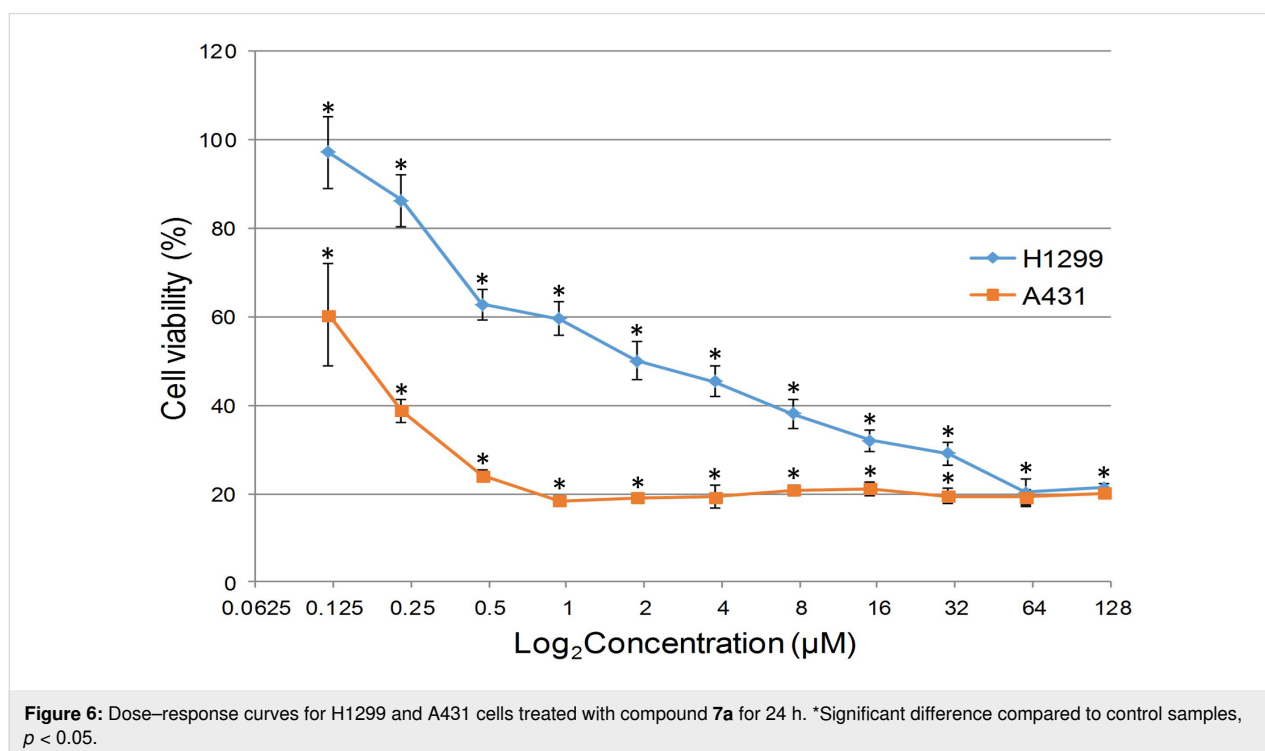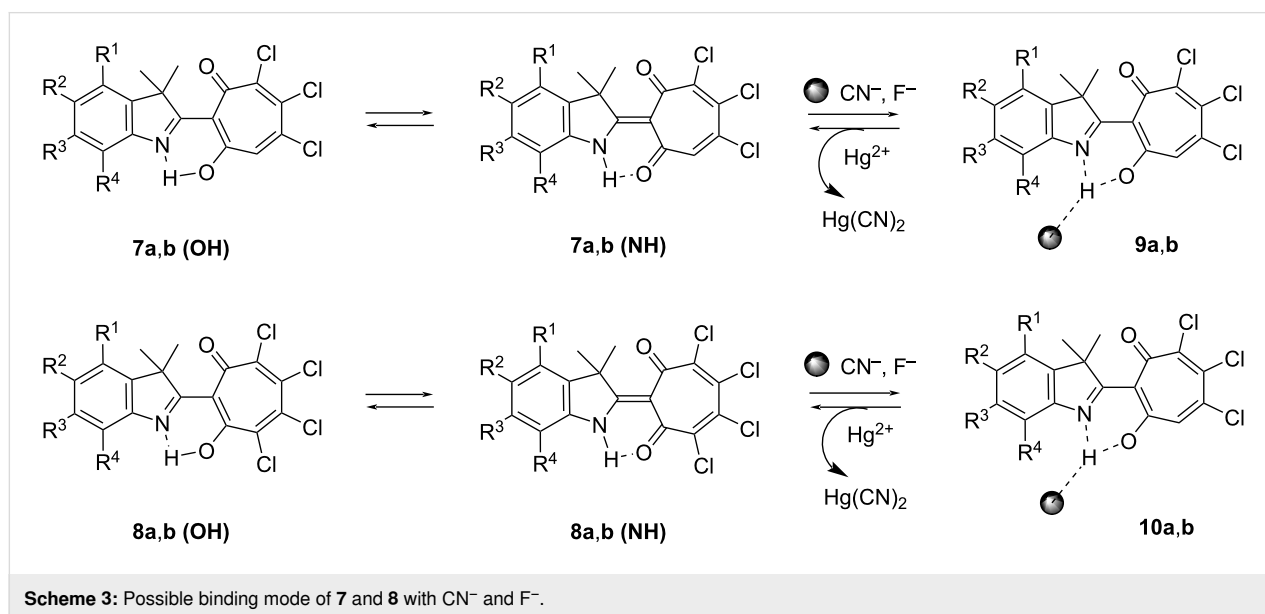

Figure 5: Absorption and emission spectra of compound **8b** in acetonitrile before (*1,1'*) (*c* 2.5 × 10^{-5} mol L^{-1}) and after the addition of CN$^-$ (*2,2'*) and F$^-$ (*3,3'*) ions (*c* 5.0 × 10^{-5} mol L^{-1}).

to different cations. It appeared that the addition of an equivalent amount of $Hg(ClO_4)_2$ to an acetonitrile solution selectively and completely restores the initial absorption and fluorescence spectra (Scheme 3).

Thus, the obtained compounds represent molecular switches of optical and fluorescent properties under sequential addition of CN^- and Hg^{2+} ions and the transformation cycle presented in Scheme 3 can be repeated at least 5–6 times.

The resulting compounds **7b** and **8a,b** have extremely low water solubility, which makes it impossible to prepare concentrations sufficient for studying cellular cytotoxicity. In this regard, 1,3-tropolone **7a**, which has an acceptable level of solubility in water, was used for biological testing. The in vitro cytotoxic activity was investigated with A431 skin cancer and H1299 lung cancer cell lines. A standard MTT assay was used to determine the anticancer activity of compound **7a** against these cultures (Figure 6). The viability test is an impor-

Scheme 3: Possible binding mode of **7** and **8** with CN^- and F^-.

Figure 6: Dose–response curves for H1299 and A431 cells treated with compound **7a** for 24 h. *Significant difference compared to control samples, $p < 0.05$.

tant method to determine which new compounds are able to target cancer cells. The results of this test (IC$_{50}$ value ± 95% confidence interval) allow us to evaluate the possibility of carrying out subsequent stages of research and selecting promising compounds for the further development of anticancer drugs [30].

The study showed that the IC$_{50}$ inhibitory concentration of 2-(1,1-dimethyl-1*H*-benzo[*e*]indolin-2-yl)-5,6,7-trichloro-1,3-tropolone (**7a**) against the A431 skin cancer cell culture, at which the number of live cells was reduced by 50%, was 0.172 ± 0.029 µM. For the H1299 culture, this value was 2.18 ± 0.7 µM. In comparison, the IC$_{50}$ value of the standard anticancer drug cisplatin at 24 hour incubation is 137 ± 12 µM for the A431 culture [31] and 34.9 µM for the H1299 culture [32], which is significantly higher than the values obtained for compound **7a**.

Conclusion

In summary, new 2-(benzo[*e*(*g*)]indolin-2-yl)-5,6,7-trichloro-1,3-tropolones **7a,b** and 2-(benzo[*e*(*g*)]indolin-2-yl)-4,5,6,7-tetrachloro-1,3-tropolones **8a,b** were obtained by acid-catalyzed reactions of benzo[*e*(*g*)] derivatives of 2,3,3-trimethylindolenines with *o*-chloranil. The energetic characteristics of the tautomeric forms of 1,3-tropolones **7** and **8** were determined by PBE0/6-3-311+G(d,p) calculations, and the structure of 2-(3,3-dimethyl-3*H*-benzo[*g*]indolin-2-yl)-5,6,7-trichloro-1,3-tropolone (**7b**) was established by X-ray diffraction analysis. Using two-dimensional correlation NMR spectroscopy methods, it was shown that the nature of the solvent significantly affects the equilibrium of the tautomeric forms of the 1,3-tropolones. The obtained compounds represent molecular switches of optical and fluorescent properties under sequential addition of CN⁻ and Hg²⁺ ions. 2-(1,1-Dimethyl-1*H*-benzo[*e*]indolin-2-yl)-5,6,7-trichloro-1,3-tropolone (**7a**) was found to exhibit high in vitro cytotoxic activity against A431 skin cancer and H1299 lung cancer cell lines. In addition, the IC$_{50}$ values of compound **7a** are significantly lower than the IC$_{50}$ values of cisplastin, which is widely used in the therapy of tumors, including lung cancer.

Experimental
General

^{1}H, ^{13}C and ^{15}N NMR spectra were obtained on the integrated analytical LC–SPE–NMR–MS system AVANCE-600 (Bruker) (600 MHz, ^{1}H; 150 MHz, ^{13}C; 60 MHz, ^{15}N) at 20 °C in CDCl$_3$ and DMSO-d_6. The signals were referenced to the signals of residual proton signals of corresponding deutero-solvents. IR spectra were recorded on a Varian Excalibur 3100 FTIR instrument using the attenuated total internal reflection technique. Mass spectra were obtained on a Finnigan Mat Incos

50 spectrometer. Electronic absorption spectra were obtained on a Varian Cary 100 spectrophotometer. Emission spectra were recorded on a Varian Cary Eclipse spectrofluorimeter. Acetonitrile of spectroscopic grade (Aldrich), previously purified by distillation, and tetra-*n*-butylammonium salts (TBAX: F, Cl, Br, I, CN) (Aldrich) were used to prepare the solutions. Spectral fluorescent experiments were performed using quartz cells ($l_{cuvette}$ 1.0 cm, volume V 2 mL). Stock solutions of compounds **7** or **8** (c 5.0 × 10⁻⁵ mol L⁻¹) and tetrabutylammonium salts (c 1.0 × 10⁻⁴ mol L⁻¹) in acetonitrile were used. The corresponding solution (1 mL) and the tetra-*n*-butylammonium salt (1 mL) solution were mixed directly in the cell and thoroughly stirred. Hence, the working concentrations of compounds **7** or **8** and anions was 2.5 × 10⁻⁵ mol L⁻¹ and 5.0 × 10⁻⁵ mol L⁻¹, respectively. All spectral experiments were performed at room temperature (23 °C). Chromatography was carried out on columns filled with Al$_2$O$_3$ of II–III degree of activity according to Brockmann. Melting points were determined on a Fisher-Johns melting point apparatus. 1,1,2-Trimethyl-1*H*-benzo[*e*]indolenine (**2a**, 98%, Alfa Aesar), 2,3,3-trimethyl-3*H*-benzo[*g*]indolenine (**2b**, 98%, Alfa Aesar) and tetrachloro-*o*-benzoquinone (*o*-chloranil, **3**) (97%, ACROS organics) were used as the starting reagents. NMR and IR spectra were recorded on the equipment of the Center for Collective Usage "Molecular Spectroscopy" of Southern Federal University.

X-ray diffraction study

The unit cell parameters and reflection intensities for compound **7b** (a three-dimensional set) were measured on an Xcalibur EOS autodiffractometer (Mo Kα irradiation, graphite monochromator, 150 K). Orange monoclinic crystals, chemical formula C$_{21}$H$_{14}$NO$_2$Cl$_3$, M = 418.68, a = 11.4480(3), b = 7.4883(2), c = 21.7720(6) Å, β = 102.590(3)°, V = 1821.55(9) Å^3, Z = 4, ρ$_{calc}$ = 1.527 g cm⁻³, µ(Mo Kα) = 0.520 mm⁻¹, $P2_1/c$ space group. Intensities of 15441 reflections were measured in the reciprocal space (2θ ≤ 64.14°) using the ω/2θ-scanning method from a single crystal with dimensions of 0.31 × 0.25 × 0.20 mm. An empirical accounting of absorption was carried out using the Multiscan procedure. After exclusion of systematically cancelled reflections and averaging intensities of equivalent reflections, the working array of measured $F^2(hkl)$ and σ(F^2) reflections contained 6352 independent reflections, 5089 of which with $F^2 > 4\sigma(F^2)$. The structure was solved with the direct method and was refined by the full-matrix least-squares procedure (LSP) with respect to F^2 in anisotropic approximation for non-hydrogen atoms (hydrogen atoms isotropic) using the SHELXTL program. In the crystal structure, most of the H atoms are localized in the Fourier synthesis of the difference electron density, then the coordinates and isotropic thermal parameters of all H atoms were calcu-

lated by the LSP using the "rider" model [33]. The absolute shifts of all 247 varied structure parameters were less than 0.001 σ, the final value of the factor R_1 = 0.0385. The CIF file containing atomic coordinates, full tables of bond lengths, bond angles, and thermal parameters of compound **7b** have been deposited at the Cambridge Crystallographic Data Centre (CCDC 2040907) and can be obtained upon request on the website: https://www.ccdc.cam.ac.uk/data_request/cif.

Computational methods

Quantum chemical calculations were performed using the Gaussian 09 software package [34] with hybrid functional PBE0 [35,36] and 6-311+G (d,p) basis set. Solvent effects were modeled by using polarizable continuum model (PCM) [37] within the integral equation formalism (IEFPCM) [38].

Biological experiments

The MTT colorimetric test for cell viability assessment is based on the reduction by NADPH-H-dependent cellular oxidoreductase enzymes of the tetrazolium dye 3-(4,5-dimethylthiazol-2-yl)-2,5-diphenyltetrazolium bromide, which has yellow color, into violet-blue formazan, with absorption maximum in the range of 540–560 nm. The optical density of the solution in this wavelength range is an indirect indicator of the number of live cells in the culture. The cytotoxic activity of the test substance was determined by the decrease in optical density of experimental samples compared to control samples [39].

A431 and H1299 cells were seeded into 96-well plates at 15000/well in DMEM medium supplemented with 10% EFV and cultured under standard conditions at 5.0% CO_2 and 37 °C. The next day, the medium was replaced and test compound **7a** was added in a series of two-fold dilutions from 0.12 μM to 120 μM. In the control wells, the medium was replaced without adding the compound **7a**. The cells were then incubated under the same standard conditions for 24 h, after which the medium was replaced and 10% MTT solution in DMEM medium supplemented with 10% EFV was added and incubated for another 2 h under CO_2 incubator conditions. At the end of cultivation, the medium with MTT was completely removed from the wells, and the formed formazan crystals were dissolved in DMSO and the optical density of the resulting solution was measured at 540 nm. The level of cytotoxic activity was determined by the change in optical density at 540 nm in wells treated with the compound **7a** or cisplatin compared to control wells. The experiment was carried out in three biological replicates with 6 technical replicates in each. Results were analyzed using one-way ANOVA followed by Tukey's post hoc test of significance. IC_{50} values were determined in the RStudio development environment using the DRC software package [40].

Supporting Information

Supporting Information File 1
Experimental procedures and characterization data for all novel compounds **7a**, **7b**, **8a** and **8b**.
[https://www.beilstein-journals.org/bjoc/content/supplementary/1860-5397-21-26-S1.pdf]

Supporting Information File 2
^{1}H, ^{13}C NMR, IR and HRMS spectra of all novel compounds.
[https://www.beilstein-journals.org/bjoc/content/supplementary/1860-5397-21-26-S2.pdf]

Supporting Information File 3
X-ray analysis data of **7b** and DFT quantum chemical calculations for **7a**, **7b**, **8a** and **8b**.
[https://www.beilstein-journals.org/bjoc/content/supplementary/1860-5397-21-26-S3.pdf]

Supporting Information File 4
Crystallographic information file for compound **7b**.
[https://www.beilstein-journals.org/bjoc/content/supplementary/1860-5397-21-26-S4.cif]

Author Contributions
Yurii A. Sayapin: conceptualization; investigation; methodology; writing – original draft; writing – review & editing. Eugeny A. Gusakov: data curation; investigation; methodology; writing – original draft. Inna O. Tupaeva: data curation; investigation;

methodology; writing – original draft. Alexander D. Dubonosov: formal analysis; investigation; writing – review & editing. Igor V. Dorogan: investigation; writing – original draft. Valery V. Tkachev: investigation. Anna S. Goncharova: investigation; writing – original draft. Gennady V. Shilov: investigation. Natalia S. Kuznetsova: investigation. Svetlana Y. Filippova: investigation. Tatyana A. Krasnikova: investigation. Yanis A. Boumber: investigation. Alexey Y. Maksimov: investigation. Sergey M. Aldoshin: data curation; formal analysis; investigation. Vladimir I. Minkin: conceptualization; project administration; supervision.

ORCID® iDs

Yurii A. Sayapin - https://orcid.org/0000-0002-3180-1762
Eugeny A. Gusakov - https://orcid.org/0000-0001-7593-1334
Inna O. Tupaeva - https://orcid.org/0000-0002-7695-9512
Alexander D. Dubonosov - https://orcid.org/0000-0003-4701-2271
Igor V. Dorogan - https://orcid.org/0000-0002-9084-4607
Valery V. Tkachev - https://orcid.org/0000-0002-1348-1363
Anna S. Goncharova - https://orcid.org/0000-0003-0676-0871
Gennady V. Shilov - https://orcid.org/0000-0001-5279-7283
Natalia S. Kuznetsova - https://orcid.org/0000-0002-2337-326X
Svetlana Y. Filippova - https://orcid.org/0000-0002-4558-5896
Tatyana A. Krasnikova - https://orcid.org/0000-0002-1386-6490
Yanis A. Boumber - https://orcid.org/0000-0001-5003-248X
Alexey Y. Maksimov - https://orcid.org/0000-0002-9471-3903
Sergey M. Aldoshin - https://orcid.org/0000-0003-3555-7442
Vladimir I. Minkin - https://orcid.org/0000-0001-6096-503X

Data Availability Statement

All data that supports the findings of this study is available in the published article and/or the supporting information of this article.

Preprint

A non-peer-reviewed version of this article has been previously published as a preprint: doi:10.2139/ssrn.4941617

References

1. Minkin, V. I.; Aldoshin, S. M.; Komissarov, V. N.; Dorogan, I. V.; Sayapin, Y. A.; Tkachev, V. V.; Starikov, A. G. *Russ. Chem. Bull.* **2006,** *55,* 2032–2055. doi:10.1007/s11172-006-0547-x

2. Sayapin, Y. A.; Komissarov, V. N.; Bang, D. N.; Dorogan, I. V.; Minkin, V. I.; Tkachev, V. V.; Shilov, G. V.; Aldoshin, S. M.; Charushin, V. N. *Mendeleev Commun.* **2008,** *18,* 180–182. doi:10.1016/j.mencom.2008.07.002

3. Sayapin, Y. A.; Gusakov, E. A.; Kolodina, A. A.; Komissarov, V. N.; Dorogan, I. V.; Tkachev, V. V.; Shilov, G. V.; Nosova, E. V.; Aldoshin, S. M.; Charushin, V. N.; Minkin, V. I. *Russ. Chem. Bull.* **2014,** *63,* 1364–1372. doi:10.1007/s11172-014-0604-9

4. Sayapin, Y. A.; Gusakov, E. A.; Dorogan, I. V.; Tupaeva, I. O.; Teimurazov, M. G.; Fursova, N. K.; Ovchinnikov, K. V.; Minkin, V. I. *Russ. J. Bioorg. Chem.* **2016,** *42,* 224–228. doi:10.1134/s1068162016020114

5. Sayapin, Y. A.; Tupaeva, I. O.; Kolodina, A. A.; Gusakov, E. A.; Komissarov, V. N.; Dorogan, I. V.; Makarova, N. I.; Metelitsa, A. V.; Tkachev, V. V.; Aldoshin, S. M.; Minkin, V. I. *Beilstein J. Org. Chem.* **2015,** *11,* 2179–2188. doi:10.3762/bjoc.11.236

6. Gusakov, E. A.; Topchu, I. A.; Mazitova, A. M.; Dorogan, I. V.; Bulatov, E. R.; Serebriiskii, I. G.; Abramova, Z. I.; Tupaeva, I. O.; Demidov, O. P.; Toan, D. N.; Lam, T. D.; Bang, D. N.; Boumber, Y. A.; Sayapin, Y. A.; Minkin, V. I. *RSC Adv.* **2021,** *11,* 4555–4571. doi:10.1039/d0ra10610k

7. Kit, O. I.; Minkin, V. I.; Lukbanova, E. A.; Sayapin, Y. A.; Gusakov, E. A.; Sitkovskaya, A. O.; Filippova, S. Y.; Komarova, E. F.; Volkova, A. V.; Khodakova, D. V.; Mindar, M. V.; Lazutin, Y. N.; Engibaryan, M. A.; Kolesnikov, V. E. *Bull. Sib. Med.* **2022,** *21,* 60–66. doi:10.20538/1682-0363-2022-2-60-66

8. Johns, R. B.; Johnson, A. W. *Chem. Ind.* **1954,** 192–193.

9. Chapman, O. L.; Fitton, P. *J. Am. Chem. Soc.* **1963,** *85,* 41–47. doi:10.1021/ja00884a008

10. Becker, A. M.; Rickards, R. W. *Org. Prep. Proced. Int.* **1983,** *15,* 239–242. doi:10.1080/00304948309356648

11. Rahman, M. M.; Matano, Y.; Suzuki, H. *J. Chem. Soc., Perkin Trans. 1* **1999,** 1533–1542. doi:10.1039/a900751b

12. Zinser, H.; Henkel, S.; Föhlisch, B. *Eur. J. Org. Chem.* **2004,** 1344–1356. doi:10.1002/ejoc.200300600

13. Schenck, G. O.; Brähler, B.; Cziesla, M. *Angew. Chem.* **1956,** *68,* 247–248. doi:10.1002/ange.19560680707

14. Kogler, H.; Fehlhaber, H.-W.; Leube, K.; Dürckheimer, W. *Chem. Ber.* **1989,** *122,* 2205–2206. doi:10.1002/cber.19891221123

15. Li, H.; Li, W.; Li, Z. *Chem. Commun.* **2009,** 3264–3266. doi:10.1039/b903515j

16. Mondal, A.; Hazra, R.; Grover, J.; Raghu, M.; Ramasastry, S. S. V. *ACS Catal.* **2018,** *8,* 2748–2753. doi:10.1021/acscatal.8b00397

17. Chien, P.-C.; Chen, Y.-R.; Chen, Y.-J.; Chang, C.-F.; Marri, G.; Lin, W. *Adv. Synth. Catal.* **2024,** *366,* 420–425. doi:10.1002/adsc.202301344

18. Humphrey, G. R.; Kuethe, J. T. *Chem. Rev.* **2006,** *106,* 2875–2911. doi:10.1021/cr0505270

19. Shiri, M. *Chem. Rev.* **2012,** *112,* 3508–3549. doi:10.1021/cr2003954

20. Lygin, A. V.; de Meijere, A. *Angew. Chem., Int. Ed.* **2010,** *49,* 9094–9124. doi:10.1002/anie.201000723

21. Zhuo, C.-X.; Zhang, W.; You, S.-L. *Angew. Chem., Int. Ed.* **2012,** *51,* 12662–12686. doi:10.1002/anie.201204822

22. Bandini, M.; Eichholzer, A. *Angew. Chem., Int. Ed.* **2009,** *48,* 9608–9644. doi:10.1002/anie.200901843

23. Sayapin, Y. A.; Tupaeva, I. O.; Gusakov, E. A.; Shilov, G. V.; Tkachev, V. V.; Aldoshin, S. M.; Minkin, V. I. *Dokl. Chem.* **2015,** *460,* 33–36. doi:10.1134/s0012500815020019

24. Sayapin, Y. A.; Dorogan, I. V.; Gusakov, E. A.; Bang, D. N.; Tkachev, V. V.; Tupaeva, I. O.; Tran, D. L.; Nguyen, T. V.; Duong, T. N.; Dinh, H. V.; Krasnikova, T. A.; Aldoshin, S. M.; Minkin, V. I. *ACS Omega* **2021,** *6,* 18226–18234. doi:10.1021/acsomega.1c02033

25. Sayapin, Y. A.; Duong, B. N.; Komissarov, V. N.; Dorogan, I. V.; Makarova, N. I.; Bondareva, I. O.; Tkachev, V. V.; Shilov, G. V.; Aldoshin, S. M.; Minkin, V. I. *Tetrahedron* **2010,** *66,* 8763–8771. doi:10.1016/j.tet.2010.08.077

26. Joshi, H. C.; Antonov, L. *Molecules* **2021,** *26,* 1475. doi:10.3390/molecules26051475

27. Kwon, J. E.; Park, S. Y. *Adv. Mater. (Weinheim, Ger.)* **2011,** *23,* 3615–3642. doi:10.1002/adma.201102046

28. Kaur, N.; Kaur, G.; Fegade, U. A.; Singh, A.; Sahoo, S. K.; Kuwar, A. S.; Singh, N. *TrAC, Trends Anal. Chem.* **2017,** *95,* 86–109. doi:10.1016/j.trac.2017.08.003

29. Suganya, S.; Naha, S.; Velmathi, S. *ChemistrySelect* **2018,** *3,* 7231–7268. doi:10.1002/slct.201801222

30. Bai, L.; Gao, C.; Liu, Q.; Yu, C.; Zhang, Z.; Cai, L.; Yang, B.; Qian, Y.; Yang, J.; Liao, X. *Eur. J. Med. Chem.* **2017,** *140,* 349–382. doi:10.1016/j.ejmech.2017.09.034

31. Bannon, J. H.; Fichtner, I.; O'Neill, A.; Pampillón, C.; Sweeney, N. J.; Strohfeldt, K.; Watson, R. W.; Tacke, M.; Mc Gee, M. M. *Br. J. Cancer* **2007,** *97,* 1234–1241. doi:10.1038/sj.bjc.6604021

32. Tang, Z.; Du, W.; Xu, F.; Sun, X.; Chen, W.; Cui, J.; Tang, W.; Yang, F.; Teng, F.; Lin, J.; Liu, B.; Dong, J. *Int. J. Biol. Sci.* **2022,** *18,* 2060–2074. doi:10.7150/ijbs.66630

33. *SHELXTL; Structure Determination Software Suite,* Version 6.14; Bruker AXS: Madison, Wisconsin, USA, 2000.

34. *Gaussian 09,* Revision A.01; Gaussian, Inc.: Wallingford, CT, 2009.

35. Perdew, J. P.; Burke, K.; Ernzerhof, M. *Phys. Rev. Lett.* **1996,** *77,* 3865–3868. doi:10.1103/physrevlett.77.3865

36. Adamo, C.; Barone, V. *J. Chem. Phys.* **1999,** *110,* 6158–6170. doi:10.1063/1.478522

37. Barone, V.; Cossi, M.; Tomasi, J. *J. Chem. Phys.* **1997,** *107,* 3210–3221. doi:10.1063/1.474671

38. Cancès, E.; Mennucci, B.; Tomasi, J. *J. Chem. Phys.* **1997,** *107,* 3032–3041. doi:10.1063/1.474659

39. Mosmann, T. *J. Immunol. Methods* **1983,** *65,* 55–63. doi:10.1016/0022-1759(83)90303-4

40. Ritz, C.; Baty, F.; Streibig, J. C.; Gerhard, D. *PLoS One* **2015,** *10,* e0146021. doi:10.1371/journal.pone.0146021